P-WAVE DIFFRACTION AND REFLECTION TRAVELTIMES FOR A HOMOGENEOUS 3D TTI MEDIUM

QI HAO and ALEXEY STOVAS

Norwegian University of Science and Technology (NTNU), Department of Petroleum Engineering and Applied Geophysics, S.P. Andersensvei 15A, 7491 Trondheim, Norway.
qi.hao@ntnu.no, alexey.stovas@ntnu.no

(Received December 9, 2013; revised version accepted September 3, 2014)

ABSTRACT

Hao, Q. and Stovas, A., 2014. P-wave diffraction and reflection traveltimes for a homogeneous 3D TTI medium. *Journal of Seismic Exploration*, 23: 405-429.

Diffractions are produced by material discontinuities. Diffraction traveltime contains information about the velocity along the entire ray path, which is useful for improving the image quality. We derive an analytical midpoint-offset diffraction traveltime approximation for P-waves in a 3D homogeneous transversely isotropic medium with a tilted symmetry axis (TTI) under the assumption of weak anellipticity of the medium. From the proposed diffraction traveltime approximation, we also derive the P-wave reflection traveltime for a dip-constrained transversely isotropic (DTI) model. Two numerical examples illustrate the accuracy of both approximations for diffraction and reflection traveltime. One example is provided to analyze the shape of midpoint-offset diffraction traveltime. A short discussion on possible applications in heterogeneous TTI and multi-layered DTI models concludes the paper.

KEY WORDS: diffraction, traveltime, anisotropy.

INTRODUCTION

The diffracted wave in a seismic record includes information on small scale discontinuities of the subsurface. Diffraction can be used in high-resolution imaging, local velocity analysis, etc. The diffraction traveltime in homogeneous anisotropic media can be represented in form of a double-square-root (DSR) equation, which is also valid for media with moderate lateral velocity variation (Landa and Keydar, 1998; Dell et al., 2013). The DSR equation, Cheop's equivalent pyramid, is widely used to implement the Kirchhoff time migration

0963-0651/14/$5.00

in isotropic media (Claerbout, 1985, p.164-166; Alkhalifah, 2000b). Alkhalifah (2000b) derived the Cheops' pyramid for homogeneous transversely isotropic media with a vertical symmetry axis (VTI).

In this paper, we derive an analytical approximation for midpoint-offset P-wave diffraction traveltime from a point diffractor in a 3D TTI medium under the assumption of weak anellipticity of the medium. In the derived diffraction traveltime equation, both source and receiver slownesses are analytically approximated by a combination of Taylor expansion with respect to the anellipticity parameter and its Shanks transform (Bender and Orszag, 1978). This technique is first used by Alkhalifah (2000b) to obtain the midpoint-offset traveltime approximation for VTI media. Recently, similar techniques were applied to derive the offset-midpoint traveltime equations for 2D TTI (Hao and Stovas, 2013; Stovas and Alkhalifah, 2013) and 3D horizontal transversely isotropic (HTI) media (Hao et al., 2013). As a straightforward consequence of the diffraction traveltime approximation, the P-wave reflection traveltime is derived for a 3D homogeneous dip-constrained transversely isotropic (DTI) model (i.e., TI medium with the symmetry axis orthogonal to the reflector). Reflection moveout approximation has proved helpful in anisotropic velocity model-building (e.g. Grechka et al., 2002; Tsvankin and Grechka, 2011). In recent years, there has been a significant progress in extending reflection traveltime tomography to TTI media (Bakulin et al., 2010; Zhou et al., 2011; Wang and Tsvankin, 2013a, 2013b).

This paper is organized as follows: we start with the exact diffraction traveltime represented in terms of source and receiver slownesses in a general anisotropic medium for a TTI medium. In the following section, we derive the analytical slowness approximation. Then, we obtain the reflection traveltime for P-wave in a 3D homogeneous DTI model from the midpoint-offset diffraction traveltime approximation for 3D TTI media. The accuracies of the proposed diffraction and reflection traveltime formulas are tested on homogeneous transversely isotropic (TI) models. At the end, we briefly discuss the application of the proposed approximation in calculating P-wave diffraction and reflection traveltime for heterogeneous TTI media and the multi-layered DTI media.

EXACT DIFFRACTION TRAVELTIME IN A HOMOGENOUS ANISOTROPIC MEDIUM

We consider a general anisotropic homogeneous medium with the acquisition geometry shown in Fig. 1. The position of the single diffractor is denoted by (x_1, x_2, z). The exact diffraction traveltime for P-wave in this medium is a sum of the source-diffractor traveltime and the receiver-diffractor traveltime,

$$T = |q_S z + p_{S1} y_{S1} + p_{S2} y_{S2}| + |q_g z + p_{g1} y_{g1} + p_{g2} y_{g2}| \quad , \tag{1}$$

where (y_{S1}, y_{S2}) denote projections of the lateral distance between the diffractor and the source given by $(y_{S1}, y_{S2}) = (x_1 - m_1 + h_1, x_2 - m_2 + h_2)$ and (y_{g1}, y_{g2}) denotes projections of the lateral distance between the diffractor and the receiver given by $(y_{g1}, y_{g2}) = (x_1 - m_1 - h_1, x_2 - m_2 - h_2)$. The vectors $(p_{S1}, p_{S2}, -q_S)$ and $(p_{g1}, p_{g2}, -q_g)$ are the source and receiver slownesses and satisfy the following conditions,

$$\partial q / \partial p_1 = -y_1 / z \quad , \tag{2}$$

$$\partial q / \partial p_2 = -y_2 / z \quad . \tag{3}$$

Here, (p_1, p_2, q) and (y_1, y_2) are either (p_{S1}, p_{S2}, q_S) and (y_{S1}, y_{S2}) for source or (p_{g1}, p_{g2}, q_g) and (y_{g1}, y_{g2}) for receiver.

Eqs. (1)-(3) apply to the P-wave diffraction traveltime in source-receiver and midpoint-offset domains.

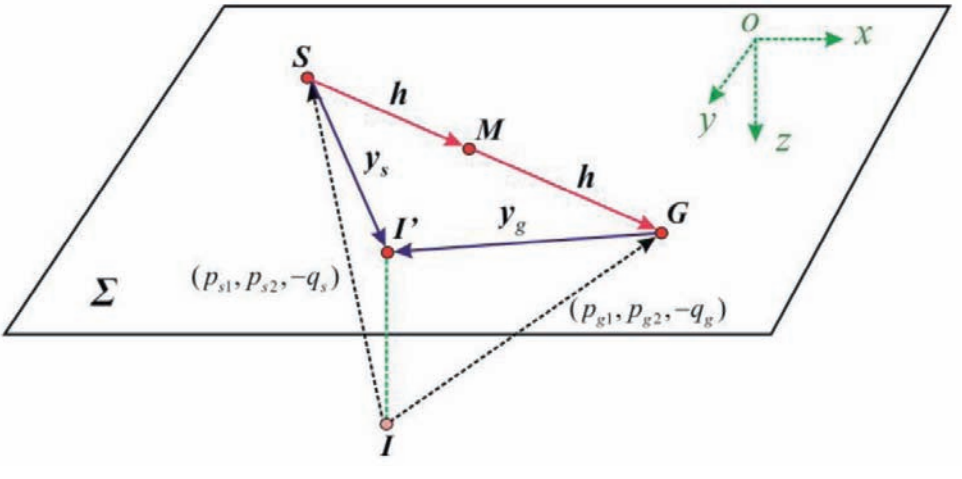

Fig. 1. Acquisition geometry for diffracted P-waves in a homogeneous anisotropic medium. Source **S**, receiver **G** and midpoint **M** = $(m_1, m_2, 0)$ are located on surface **Σ**. The half-offset vector **h** = (h_1, h_2) equals a half of the distance vector from source **S** to receiver **G**. Point **I** = (x_1, x_2, z) denotes a diffractor. Point **I′** = $(x_1, x_2, 0)$ is the projection of diffractor **I** on surface **Σ**. Vector $\mathbf{y}_s = (y_{s1}, y_{s2})$ denotes the lateral distance from source **S** to diffractor **I**, and vector $\mathbf{y}_g = (y_{g1}, y_{g2})$ denotes the lateral distance from receiver **G** to image point **I**. The seismic rays **IS** and **IG** have source slowness $(p_{s1}, p_{s2}, -q_s)$ and receiver slowness $(p_{g1}, p_{g2}, -q_g)$, respectively.

HORIZONTAL AND VERTICAL SLOWNESS APPROXIMATION

P-wave propagation in a homogeneous VTI medium is described by the vertical velocities of P- and S-waves and two Thomsen parameters, ε and δ (Thomsen, 1986; Tsvankin, 2001, p.18). In practice, we can ignore the influence of SV-wave symmetry-direction velocity on the P-wave velocity and traveltime in VTI media (Tsvankin and Thomsen, 1994; Alkhalifah, 1998). Hence, the velocity and traveltime of the P-wave in VTI media can be characterized by the vertical velocity of the P-wave v_0, the normal-moveout velocity $v_{nmo} = v_0\sqrt{(1+2\delta)}$ and the anellipticity parameter $\eta \equiv (\varepsilon-\delta)/(1+2\delta)$. Besides the three parameters mentioned above, two additional parameters, the tilt θ and azimuth φ of the symmetry axis are needed to describe 3D TTI media.

According to Alkhalifah (1998, 2000a), the 3D slowness surface for P-wave in a VTI medium in the acoustic approximation (the shear wave velocity along the symmetry axis is set to zero) is written in the following form,

$$F_{VTI} = v_0^2 q_v^2[1 - 2\eta v_{nmo}^2(p_{v1}^2+p_{v2}^2)] + (1+2\eta)v_{nmo}^2(p_{v1}^2+p_{v2}^2) - 1 = 0 , \quad (4)$$

where (p_{v1}, p_{v2}) and q_v are horizontal and vertical slowness components, respectively. The slowness surface in a TTI medium can be obtained by a simple rotation of VTI slowness surface, shown in Fig. 2. The 3D slowness surface equation for a TTI medium is obtained by applying the slowness rotation given by

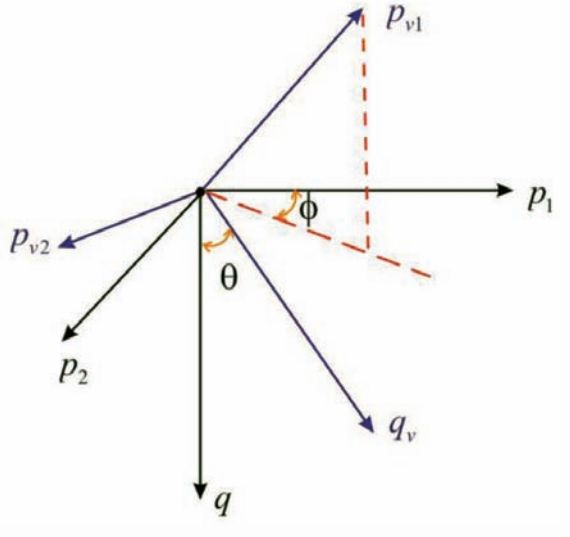

Fig. 2. Geometry of slowness coordinate system. The slownesses (p_{v1},p_{v2},q_v) correspond to a VTI medium, and (p_1,p_2,q) correspond to a TTI medium. θ denotes the tilt of the symmetry axis measured from the q-axis. φ denotes the azimuth of the symmetry axis measured from p_1 to the horizontal projection of p_{v1} on the p_1-p_2 plane. p_{v2} is located on the p_1-p_2 plane.

$$\begin{pmatrix} p_1 \\ p_2 \\ q \end{pmatrix} = \begin{pmatrix} \cos\varphi\cos\theta & -\sin\varphi & \cos\varphi\sin\theta \\ \sin\varphi\cos\theta & \cos\varphi & \sin\varphi\sin\theta \\ -\sin\theta & 0 & \cos\theta \end{pmatrix} \begin{pmatrix} p_{v1} \\ p_{v2} \\ q_v \end{pmatrix} , \tag{5}$$

where φ is the azimuth of the symmetry axis measured from the x-axis to its horizontal projection, θ is the tilt of the symmetry axis measured from the z-axis, (p_1, p_2) and q are the horizontal and vertical slowness components in the TTI medium. The P-wave slowness surface in the TTI medium is defined as

$$q = q(p_1, p_2) , \tag{6}$$

and the one for the corresponding VTI medium is

$$q_v = q_v(p_{v1}, p_{v2}) . \tag{7}$$

From eqs. (5)-(7), we derive the relationships between the slowness derivatives in VTI and TTI media (see Appendix A),

$$\partial q_v/\partial p_{v1} = -[(\partial q/\partial p_1)\cos\varphi\cos\theta + (\partial q/\partial p_2)\sin\varphi\cos\theta + \sin\theta] / [(\partial q/\partial p_1)\cos\varphi\sin\theta + (\partial q/\partial p_2)\sin\varphi\sin\theta - \cos\theta] , \tag{8}$$

$$\partial q_v/\partial p_{v2} = [(\partial q/\partial p_1)\sin\varphi - (\partial q/\partial p_2)\cos\varphi] / [(\partial q/\partial p_1)\cos\varphi\sin\theta + (\partial q/\partial p_2)\sin\varphi\sin\theta - \cos\theta] . \tag{9}$$

Substitutions of eqs. (2) and (3) into eqs. (8) and (9) results in the explicit expressions for $\partial q_v/\partial p_{v1}$ and $\partial q_v/\partial p_{v2}$,

$$\partial q_v/\partial p_{v1} = -[y_1\cos\varphi\cos\theta + y_2\sin\varphi\cos\theta - z\sin\theta] / [y_1\cos\varphi\sin\theta + y_2\sin\varphi\sin\theta + z\cos\theta] , \tag{10}$$

$$\partial q_v/\partial p_{v2} = [y_1\sin\varphi - y_2\cos\varphi] / [y_1\cos\varphi\sin\theta + y_2\sin\varphi\sin\theta + z\cos\theta] . \tag{11}$$

To derive the VTI slowness components p_{v1} and p_{v2}, we introduce the following relations,

$$p_{v1} = p_v\cos\alpha , \tag{12}$$

$$p_{v2} = p_v\sin\alpha , \tag{13}$$

where p_v denotes the magnitude of the horizontal slowness component given by

$$\partial q_v/\partial p_v = \sqrt{\{(\partial q_v/\partial p_{v1})^2 + (\partial q_v/\partial p_{v2})^2\}} = c \quad . \tag{14}$$

Here, c is a new parameter which is obtained from eqs. (10) and (11),

$$c = \sqrt{\{(y_1')^2 + (z\sin\theta - \cos\theta y_2')^2\}}/|y_2'\sin\theta + z\cos\theta| \quad , \tag{15}$$

with

$$y_1' = y_1\sin\varphi - y_2\cos\varphi \quad , \tag{16}$$

$$y_2' = y_1\cos\varphi + y_2\sin\varphi \quad , \tag{17}$$

and α denotes the azimuth of horizontal slowness projection measured from x-axis in the VTI medium, which is also obtained from eqs. (10) and (11),

$$\tan\alpha = (\partial q_v/\partial p_{v2})/(\partial q_v/\partial p_{v1}) = -[y_1\sin\varphi - y_2\cos\varphi]$$
$$/[y_1\cos\varphi\cos\theta + y_2\sin\varphi\sin\theta - z\sin\theta] \quad . \tag{18}$$

From eqs. (4) and (14), we obtain quartic equations with respect to slowness projections squared p_v^2 and q_v^2, independently,

$$p_v^2 v_{nmo}^4 - c^2 v_0^2(-1 + 2p_v^2 v_{nmo}^2\eta)^3[-1 + p_v^2 v_{nmo}^2(1+2\eta)] = 0 \quad , \tag{19}$$

$$c^2 q_v^2 v_0^4 - v_{nmo}^2(1 - q_v^2 v_0^2)(1 + 2\eta - 2q_v^2 v_0^2\eta)^3 = 0 \quad . \tag{20}$$

With the help of Taylor expansion and Shanks transform, we derive the analytical approximations for p_v^2 and q_v^2 from eqs. (19) and (20) under the weak anellipticity assumption. The final expressions for p_v^2 and q_v^2 are given in eqs. (B-9) and (B-10) in Appendix B.

ANALYTICAL APPROXIMATION FOR MIDPOINT-OFFSET DIFFRACTION TRAVELTIME

It is obvious that the peak of the Cheops' pyramid in isotropic media corresponds to the fastest ray with zero-offset. This is also valid for a single diffractor in 3D homogeneous TTI media. The surface position and the traveltime of the fastest ray are easily determined by picking the peak of the midpoint-offset traveltime pyramid. For the fastest ray, the horizontal projection of its slowness equals zero. We identify the position of the single diffractor by the fastest ray,

$$z = t_0/(2q_0) \quad , \tag{21}$$

$$x_1 = x_1^0 - z(\partial q/\partial p_1)\big|_{\substack{p_1=0 \\ p_2=0}} \quad , \tag{22}$$

$$x_2 = x_2^0 - z(\partial q/\partial p_2)\big|_{\substack{p_1=0 \\ p_2=0}} \quad , \tag{23}$$

where (x_1, x_2, z) denotes the position of the single diffractor; (x_1^0, x_2^0) and t_0 denote the surface position and two-way traveltime for the zero-offset fastest ray, respectively; $(p_1 = 0, p_2 = 0, q_0)$ denotes the slowness for the fastest ray; the vertical projection of its slowness $q_0 = q((p_1 = 0, p_2 = 0)$ is given by

$$q_0^2 = 2/[v_0^2\cos^2\theta + (1+2\eta)v_n^2\sin^2\theta + \sqrt{\{[v_0^2\cos^2\theta - (1+2\eta)v_n^2\sin^2\theta]^2 + \sin^2(2\theta)v_0^2v_n^2\}}] \quad . \tag{24}$$

Substitution of eqs. (21)-(23) into eq. (1) leads to the midpoint-offset diffraction traveltime for a single diffractor in a 3D homogeneous TTI medium,

$$T = |(1/2q_0)t_0q_s + p_{s1}y_{s1} + p_{s2}y_{s2}| + |(1/2q_0)t_0q_g + p_{g1}y_{g1} + p_{g2}y_{g2}| \quad , \tag{25}$$

where (y_{s1}, y_{s2}) and (y_{g1}, y_{g2}) are represented in terms of midpoint (m_1, m_2) and offset (h_1, h_2),

$$(y_{s1}, y_{s2}) = (x_1-m_1+h_1, x_2-m_2+h_2) \quad , \tag{26}$$

$$(y_{g1}, y_{g2}) = (x_1-m_1-h_1, x_2-m_2-h_2) \quad . \tag{27}$$

Here the lateral projection of the single diffractor is represented in terms of the fastest ray,

$$x_1 = x_1^0 + (1/4q_0)t_0\zeta\sin(2\theta)\cos\varphi \quad , \tag{28}$$

$$x_2 = x_2^0 + (1/4q_0)t_0\zeta\sin(2\theta)\sin\varphi \quad , \tag{29}$$

with

$$\zeta = [-(1+2\eta)v_n^2 + v_0^2(1+2\eta q_0^2v_n^2\cos2\theta)] / [(1+2\eta)v_n^2\sin^2\theta + v_0^2(\cos^2\theta-\eta q_0^2v_n^2\sin^22\theta)] \quad . \tag{30}$$

Note that the source and receiver slownesses (p_{s1}, p_{s2}, q_s) and (p_{g1}, p_{g2}, q_g) given in eq. (25) are analytically determined in previous section in which the position (x_1, x_2, z) of the single diffractor is replaced by eqs. (21), (28) and (29).

REFLECTION TRAVELTIME IN A 3D DTI MODEL

We consider the reflection traveltime for P-wave in a 3D DTI model in which the symmetry axis is normal to the reflector. Let the reflection plane in a 3D DTI model be described in Cartesian coordinates by the general equation,

$$n_1x + n_2y + n_3z - d = 0 \quad , \tag{31}$$

where d is the normal depth from the coordinate origin to the reflector, and the unit vector $(n_1,n_2,n_3)^T$ is normal to the reflector. Since the symmetry axis in the DTI model coincides with the normal vector to the reflector, the unit vector $(n_1,n_2,n_3)^T$ is represented in terms of the azimuth φ and tilt θ of the symmetry axis,

$$(n_1,n_2,n_3)^T = (\cos\varphi\sin\theta,\sin\varphi\sin\theta,\cos\theta) \quad . \tag{32}$$

To specify the position of the reflection point, we assume that the midpoint in the acquisition system is located at the coordinate origin, the radial half-offset h and the acquisition azimuth γ measured from the x-axis (seen in Fig. 3). By considering eqs. (31) and replacing the normal depth d given in eq. (31) by the zero-offset two-way traveltime τ_0 and P-wave on-symmetry-axis velocity v_0, we derive the coordinates of the reflection point (x_R,y_R,z_R) given by

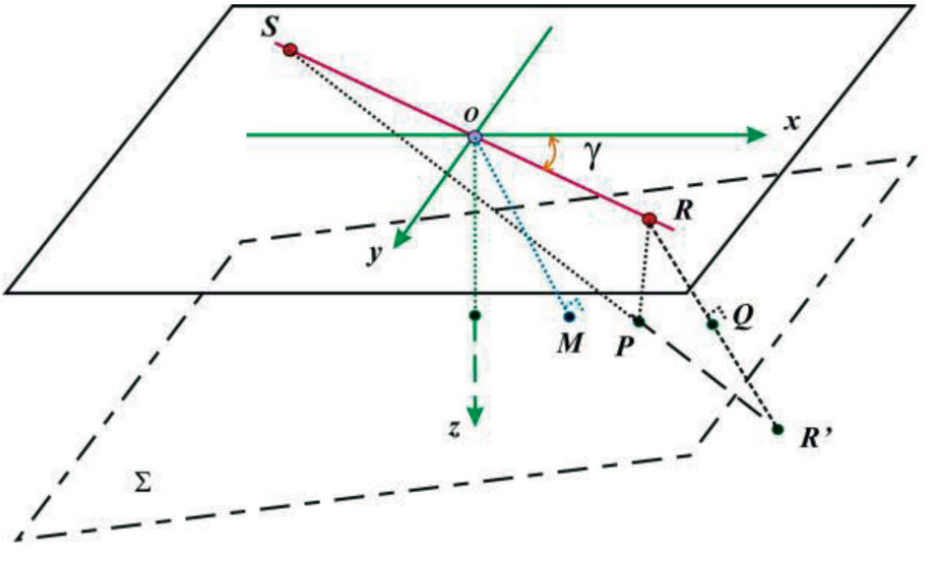

Fig. 3. Schematic plot of reflection ray SPR in a DTI model. Symbols S, O, and R denote source, midpoint and receiver, respectively. Line segment OM denotes the zero-offset ray, which is normal to reflector Σ. R′ is the image point of R with respect to the reflector Σ. Q is the midpoint of line segment RR′. γ denotes the acquisition azimuth measured from the x-axis.

$$x_R = [2h^2/(v_0\tau_0)](n_1\cos\gamma + n_2\sin\gamma)[(n_2^2+n_3^2)\cos\gamma - n_1n_2\sin\gamma] + \tfrac{1}{2}n_1v_0\tau_0 \quad ,(33)$$

$$y_R = [2h^2/(v_0\tau_0)](n_1\cos\gamma + n_2\sin\gamma)[(n_1^2+n_3^2)\sin\gamma - n_1n_2\cos\gamma] + \tfrac{1}{2}n_2v_0\tau_0 \quad ,(34)$$

$$z_R = -[2h^2/(v_0\tau_0)]n_3(n_1\cos\gamma + n_2\sin\gamma) + \tfrac{1}{2}n_3v_0\tau_0 \quad . \qquad (35)$$

By considering the offset-midpoint traveltime and the slowness approximation mentioned in previous section, we consequently derive the reflection traveltime for a P-wave in a DTI model,

$$T = 2hp_v\sqrt{\{1 - \sin^2\theta\cos^2(\gamma-\varphi)\}} + v_0\tau_0q_v \quad , \qquad (36)$$

where τ_0 is the zero-offset two-way traveltime; v_0 is the P-wave velocity along the symmetry axis; p_v and q_v are slowness projections parallel and normal to the reflector, respectively; the explicit expressions for p_v and q_v are given in equations (B-9) and (B-10) in which parameter c is given by

$$c = dq_v/dp_v = [2h/(\tau_0v_0)]\sqrt{\{1 - \sin^2\theta\cos^2(\gamma-\varphi)\}} \quad . \qquad (37)$$

Eq. (36) illustrates that the P-wave reflection traveltime in a DTI model can be represented in terms of the corresponding VTI slowness projections. Note that the maximum half-offset for reflection equation (36) is azimuth-dependent and given by

$$h_{max} = \tau_0v_0/[2\sin\theta\,|\cos(\gamma-\varphi)|] \quad . \qquad (38)$$

For a DTI model with the dip of zero, eqs. (36) and (37) are reduced to

$$T = 2hp_v + v_0\tau_0q_v \quad , \qquad (39)$$

$$c = dq_v/dp_v = 2h/\tau_0v_0 \quad , \qquad (40)$$

which correspond to the P-wave reflection traveltime for a horizontal VTI layer.

NUMERICAL EXAMPLES

In the first example, we check the accuracy of diffraction traveltime approximation (25) in homogeneous 3D TTI media. The exact traveltime is calculated by two-point ray tracing method (Reeshidev and Sen, 2005). The medium parameters are $v_0 = 2000$ m/s, $\delta = 0.2$ and $\eta = 0.2$. The azimuth of the symmetry axis is $\varphi = 0$. We change the tilt of the symmetry axis to observe its influence on the distribution of traveltime error. The lateral position of the peak (corresponding to the fastest ray) in the diffraction traveltime surface t =

$t(m_1,m_2,h_1,h_2)$ is set as $(x_1^0,x_2^0) = (0,0)$. The two-way diffraction traveltime corresponding to this peak is taken as $t_0 = 3$ s. Figs. 4-6 show the relative error of diffraction traveltime as a function of midpoint for several fixed offsets. For the case of zero-offset $(h_1,h_2) = (0,0)$, it is obvious that the tilt of the symmetry axis affects the distribution of traveltime error: relatively large error shifts towards the peak of the traveltime surface with an increase in tilt. However, this phenomenon becomes unclear for the case of nonzero-offset $(h_1,h_2) = (2\text{km},0)$ and $(h_1,h_2) = (4\text{km},0)$. From Figs. 4 to 6, we can also see that the maximum relative error is no more than 0.3%.

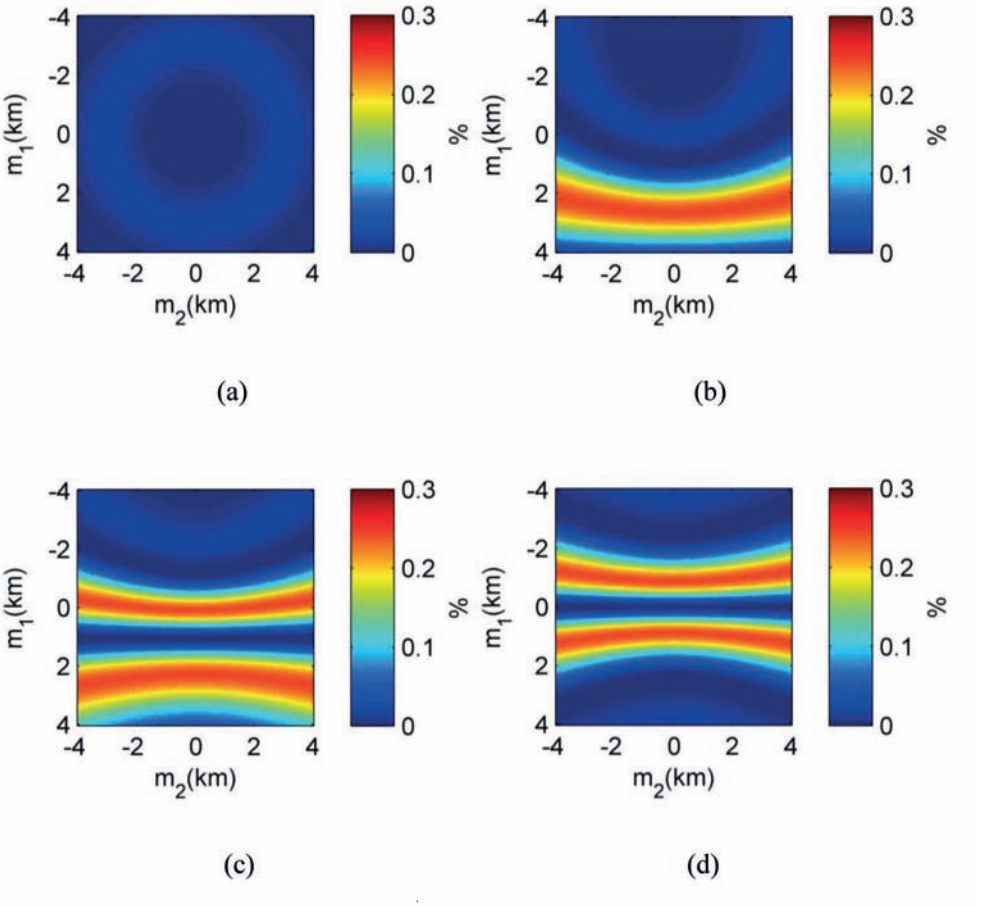

Fig. 4. Relative error in diffraction traveltime as a function of midpoint (m_1,m_2) in TTI media. In all plots, the source-receiver half-offset are kept as $(h_1,h_2) = (0,0)$. The TI medium parameters for all plots include $v_0 = 2$ km/s, $\delta = 0.2$ and $\eta = 0.2$. The azimuth of the TI symmetry is $\varphi = 0$. The tilt of the symmetry axis is $\theta = 0°$ (a), $\theta = 30°$ (b), $\theta = 60°$ (c) and $\theta = 90°$ (d), respectively. The two-way traveltime and the lateral positions for the peak in diffraction traveltime surface are taken as $t_0 = 3$ s.

In the second example, we employ eq. (25) to synthesize midpoint-offset traveltime pyramids. Fig. 7 shows the traveltime pyramids computed for different acquisition azimuth. In Fig. 7, we use the radial midpoint m and radial offset h for a specified acquisition azimuth γ. Here m and h are defined as $m = \sqrt{(m_1^2, m_2^2)}$ and $h = \sqrt{(h_1^2, h_2^2)}$, where both midpoint (m_1, m_2) and offset (h_1, h_2) correspond to acquisition azimuth γ. Only the azimuthal variation from 0° to 90° is considered, since the traveltime is symmetric with respect to y-axis for the TTI model in Fig. 7. For all plots in Fig. 7, the lateral position of the peak (corresponding to the fastest ray) in the diffraction traveltime surface is located at the origin of the (m,h) coordinate system by setting $(x_1^0, x_2^0) = (0,0)$ given in eqs. (28) and (29). Fig. 8 shows several slices extracted from the traveltime pyramids in Fig. 7 for m = 0 (common-midpoint case), h = 0 (common-offset case) and the case m = h. From both figures, we can see that the traveltime decreases as the azimuth increases and the traveltime pyramid becomes much flatter. This effect becomes more pronounced for large values of offset and midpoint.

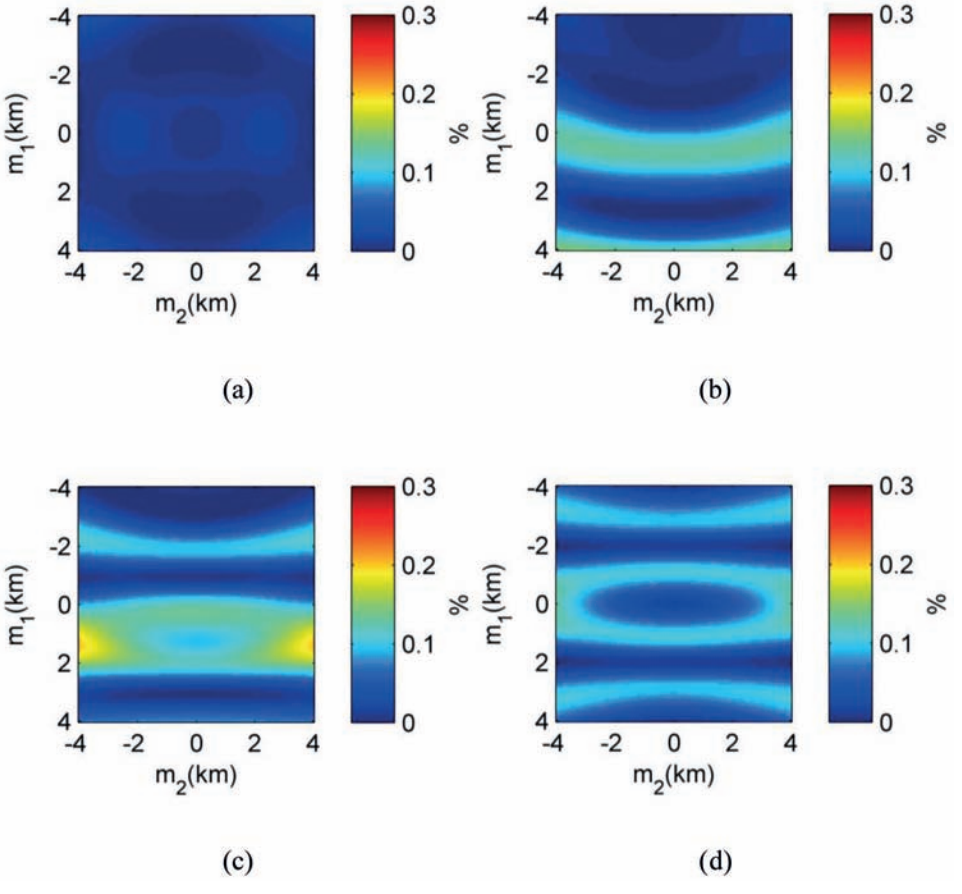

Fig. 5. Similar to Fig. 3 but the fixed half-offset is $(h_1, h_2) = (2\text{km}, 0)$.

In the last example, we test the accuracy of reflection traveltime approximation (36) in several DTI models with different dips and anellipticies. The exact traveltime is calculated by two-point ray tracing method (Reeshidev and Sen, 2005). Figs. 9-11 show the relative error of traveltime approximation (36). Note that the error curve breaks down when the corresponding offset reaches the maximum one given in eq. (38). We can see that the accuracy of reflection traveltime approximation (36) is not sensitive to the dip of the DTI model. But the value of anellipticity significantly affects the accuracy of traveltime approximation (36). By comparing the plots in Figs. 9 to 11, we can see that reflection traveltime approximation (36) has a significant error at large offsets for $\eta = 0.3$ because approximation (36) is derived under the assumption of weak anellipticity for the DTI model.

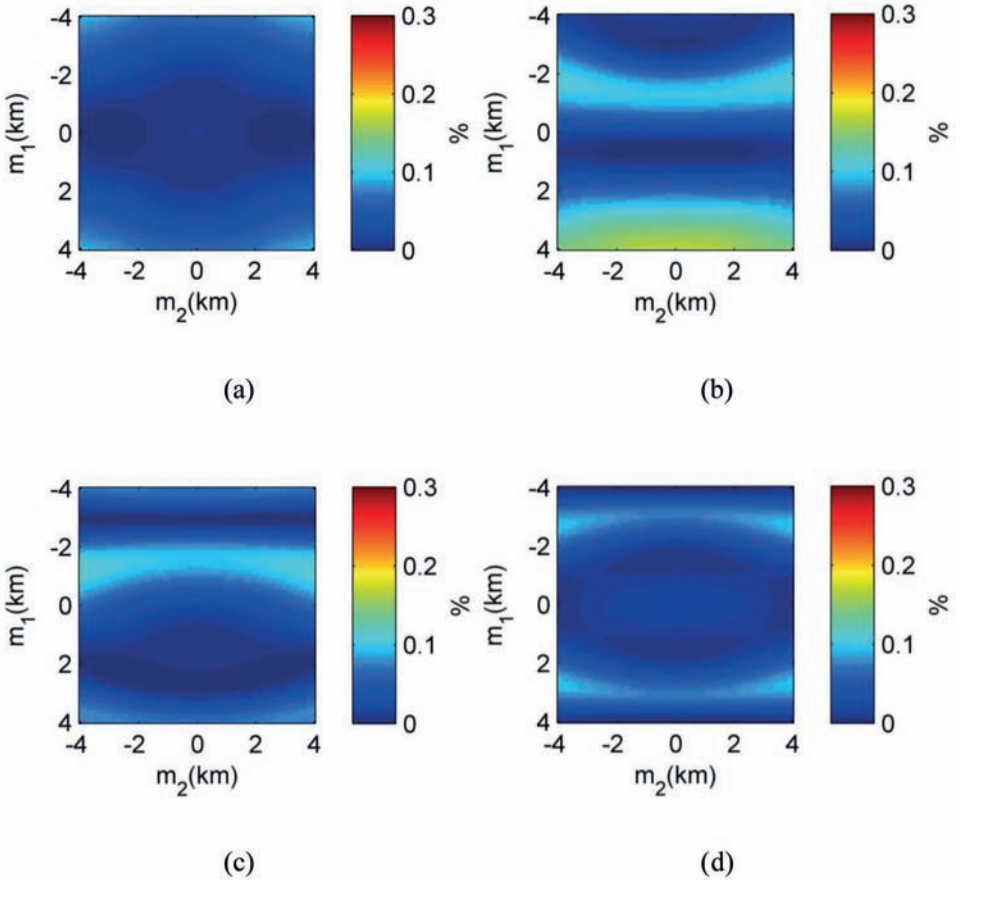

Fig. 6. Similar to Fig. 3 but the fixed half-offset is $(h_1,h_2) = (4km,0)$.

DISCUSSION

This paper introduces an analytical method to approximate P-wave diffraction traveltime in a homogeneous 3D TTI medium. For heterogeneous TTI media, the diffraction traveltime cannot be directly calculated by this method. However, the heterogeneous medium can be treated as an 'effective homogeneous' one. The effective medium parameters can be obtained by fitting the computed traveltime with the corresponding diffraction event around its peak. Obviously, the effective parameters represent the average property of a heterogeneous medium along the path of the fastest ray. The diffraction traveltime is approximately calculated by substituting the effective medium parameters into traveltime approximation (25).

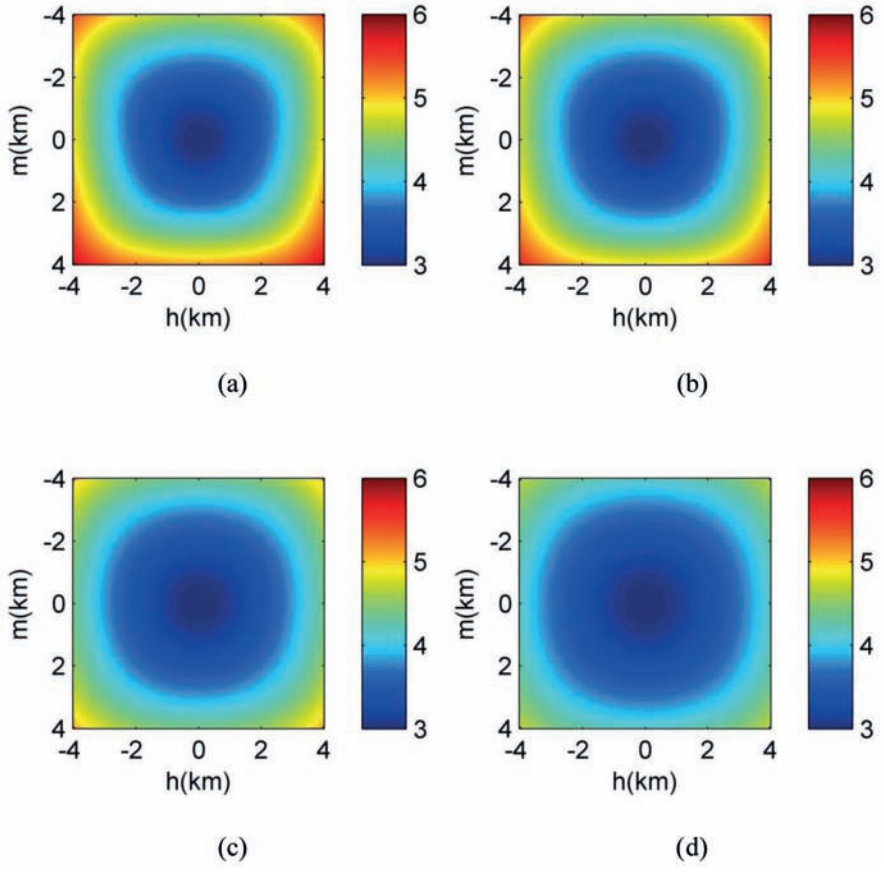

Fig. 7. Diffraction traveltime for P-wave in a 3D TTI medium as a function of half offset h and midpoint m with different acquisition azimuth $\gamma = 0°$ (a), $\gamma = 30°$ (b), $\gamma = 60°$ (c), and $\gamma = 90°$ (d). The TI medium parameters include $v_0 = 2$ km/s, $\delta = 0.2$ and $\eta = 0.2$. The tilt and the azimuth of the TI symmetry axis are $\theta = 60°$ and $\varphi = 0$, respectively.

Reflection traveltime approximation (36) is valid only for the single-layer DTI model. For the multi-layered DTI model, we derive the effective medium parameters in Appendix C. By replacing the TI medium parameters by the corresponding effective medium parameters, traveltime approximation (36) can be employed to approximately calculate the reflection traveltime for P-wave in multi-layered DTI media.

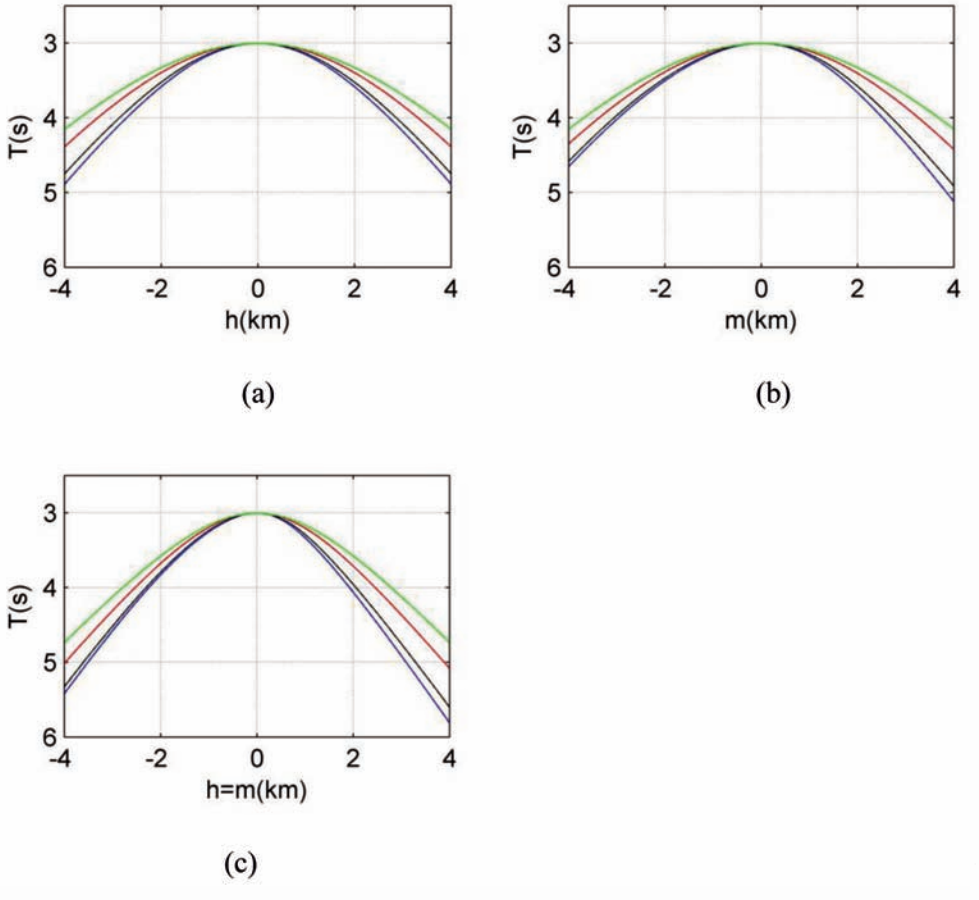

Fig. 8. Comparison of diffraction traveltimes extracted from traveltime pyramids in Fig. 7 for m = 0 (left top), h = 0 (right top) and h = m (left bottom). Blue, black, red and green lines correspond to acquisition azimuth $\gamma = 0°$, $\gamma = 30°$, $\gamma = 60°$, and $\gamma = 90°$, respectively.

CONCLUSIONS

The analytical approximation of P-wave diffraction traveltime in 3D TTI media is derived under the assumption of weak anellipticity of the model. In this approximation, the source and receiver slownesses in a TTI medium are analytically derived by rotating the approximate slowness in the corresponding VTI medium. This approximation can be useful for rapidly calculating the P-wave diffraction traveltime in the 3D TTI medium with the weak or moderate anellipticity ($\eta \leq 0.2$).The derived reflection traveltime approximation is also valid at large offset for the homogeneous DTI model with the weak or moderate anellipticity ($\eta \leq 0.2$).

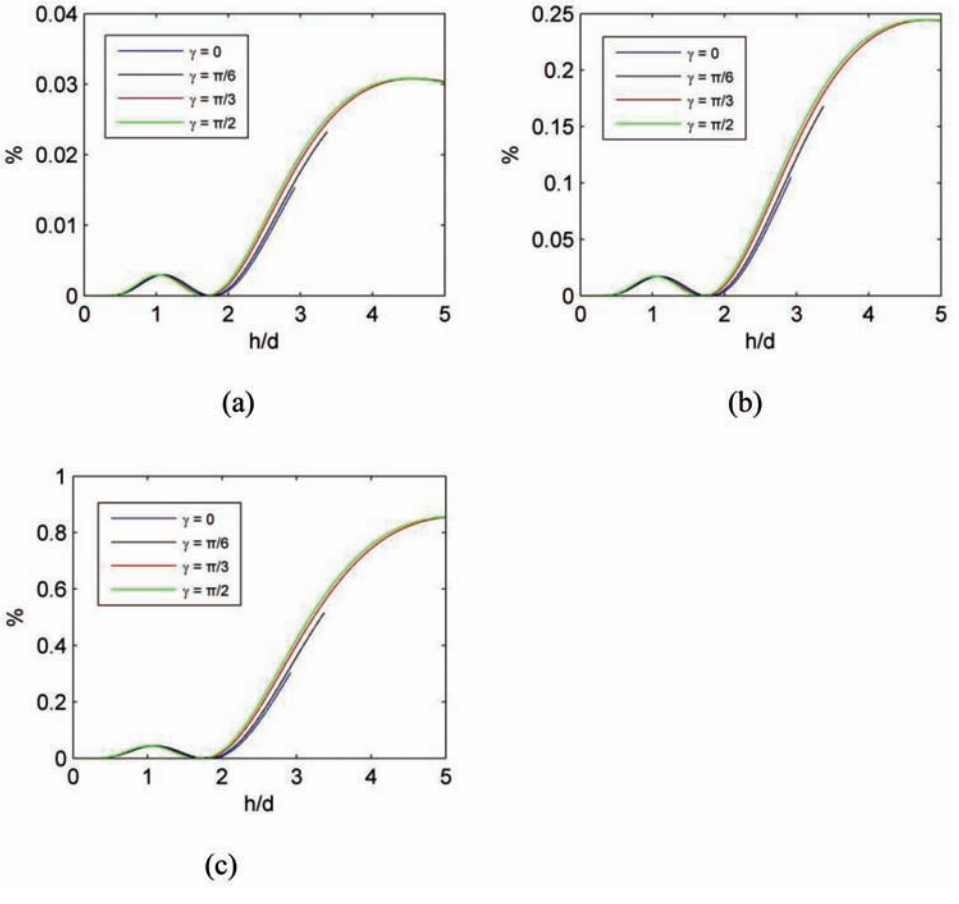

Fig. 9. Relative error of the reflection traveltime eq. (36) as a function of the normalized half-offset (the ratio of half-offset h to the normal depth d in the DTI model) in three 3D DTI models with $\eta = 0.1$ (a), $\eta = 0.2$ (b), $\eta = 0.3$ (c). γ denotes the acquisition azimuth measured from the x-axis. In all models, the zero-offset two-way traveltime is taken as $\tau = 3$ s; the TI medium parameters are $v_0 = 2$ km/s, $\delta = 0.2$; the azimuth and the tilt of the TI symmetry axis are $\varphi = 0$ and $\theta = 20°$, respectively.

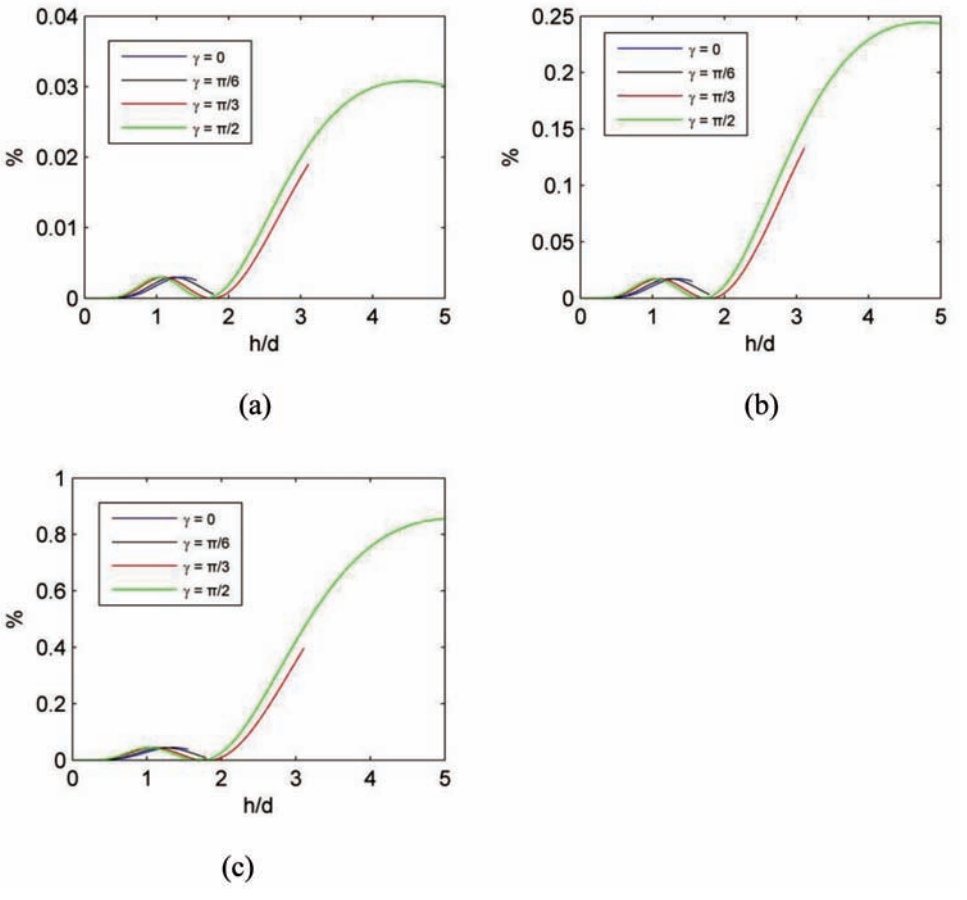

Fig. 10. Similar to Fig. 9 but the tilt of the TI symmetry axis is $\theta = 40°$.

ACKNOWLEDGEMENTS

We would like to acknowledge the ROSE project for financial support. We also acknowledge an anonymous reviewer for many valuable remarks.

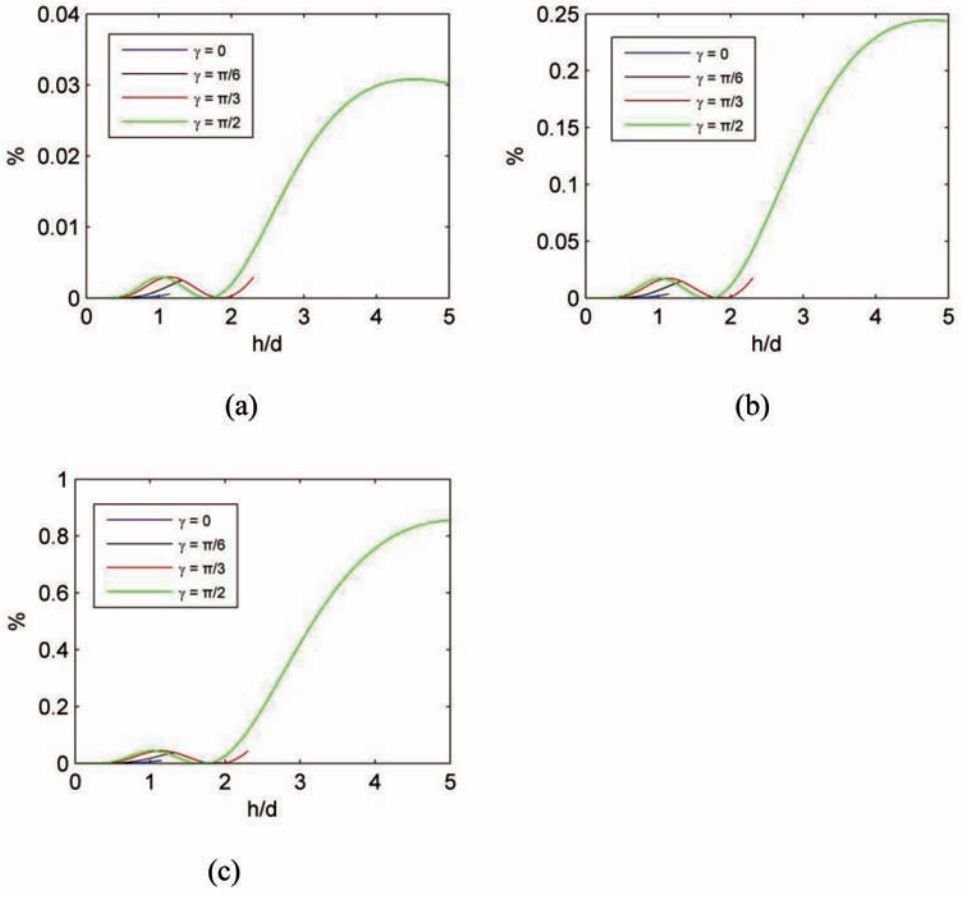

Fig. 11. Similar to Fig. 9 but the tilt of the TI symmetry axis is $\theta = 60°$.

REFERENCES

Alkhalifah, T., 1998. Acoustic approximations for seismic processing in transversely isotropic media. Geophysics, 63: 623-631.

Alkhalifah, T., 2000a. An acoustic wave equation for anisotropic media. Geophysics, 65: 1239-1250.

Alkhalifah, T., 2000b. The offset-midpoint traveltime pyramid in transversely isotropic media. Geophysics, 65: 1316-1325.

Bender, C.M. and Orszag, S.A., 1978. Advanced Mathematical Methods for Scientists and Engineers. McGraw-Hill, New York.

Bakulin, A., Woodward, M., Nichols, D., Osypov, K. and Zdraveva, O., 2010. Building tilted transversely isotropic depth models using localized anisotropic tomography with well information. Geophysics, 75, D27-D36.

Claerbout, J., 1985. Imaging the Earth's Interior. Blackwell Science Inc., New York.

Dell, S., Pronevich, A., Kashtan, B. and Grajewski, D., 2013. Diffraction traveltime approximation for general anisotropic media. Geophysics, 78: WC15-WC23.
Fomel, S. and Stovas, A., 2010. Generalized nonhyperbolic moveout approximation. Geophysics, 75: U9-U18.
Grechka, V., Pech, A. and Tsvankin, I., 2002. Multicomponent stacking-velocity tomography for transversely isotropic media. Geophysics, 67: 1564-1574.
Hao, Q. and Stovas, A., 2013. The offset-midpoint traveltime pyramid in TTI media. Extended Abstr., 75th EAGE Conf., London: P01 05.
Hao, Q., Stovas, A. and Alkhalifah T., 2013. The azimuth-dependent offset-midpoint traveltime pyramid in 3D HTI media. Expanded Abstr, 83rd Ann. Internat. SEG Mtg., Houston. doi: 10.1190/segam2013-0058.1.
Landa, E. and Keydar, S., 1998. Seismic monitoring of diffraction images for detection of local heterogeneities. Geophysics, 63: 1093-1100.
Reeshidev, B. and Sen, M.K., 2005. 3-D two-point ray tracing in general anisotropic media. Expanded Abstr., 75th Ann. Internat. SEG Mtg., Houston: 190-193.
Stovas, A. and Alkhalifah, T., 2013. Mapping moveout approximations in TI media. Geophysics, 79: C19-C26.
Thomsen, L., 1986. Weak elastic anisotropy. Geophysics, 51: 1954-1966.
Tsvankin, I. and Thomsen, L., 1994. Nonhyperbolic reflection moveout in anisotropic media. Geophysics, 59: 1290-1304.
Tsvankin, I., 2001. Seismic Signatures and Analysis of Reflection Data in Anisotropic Medium. Elsevier Science Publishers, Amsterdam.
Tsvankin, I. and Grechka, V., 2011. Seismology of Azimuthally Anisotropic Media and Seismic Fracture Characterization. SEG, Tulsa, OK.
Ursin, B. and Stovas, A., 2006. Traveltime approximations for a layered transversely isotropic medium. Geophysics, 71: D23-D33.
Wang, X., and Tsvankin, I., 2011. Moveout inversion of wide-azimuth P-wave data for tilted TI media. Geophysics, 76, WA23-WA29.
Wang, X. and Tsvankin, I., 2013a. Ray-based gridded tomography for tilted transversely isotropic media. Geophysics, 78, C11-C23.
Wang, X. and Tsvankin, I., 2013b. Multiparameter TTI tomography of P-wave reflection and VSP data. Geophysics, 78, WC51-WC63.
Woodward, M.J., Nichols, D., Zdraveva, O., Whitfield, P. and Johns, T., 2008. A decade of tomography. Geophysics, 73: VE5-VE11.
Zhou, C., Jiao, J., Lin, S., Sherwood, J. and Brandsberg-Dahl, S., 2011. Multiparameter joint tomography for TTI model building. Geophysics, 76: WB183-WB190.

APPENDIX A

THE RELATIONS OF SLOWNESS DERIVATIVES BETWEEN VTI AND TTI MEDIA

In this appendix, we derive the relations of slowness derivatives between VTI and TTI media. The perturbation of eq. (5) is written in the form,

$$\begin{pmatrix} \Delta p_1 \\ \Delta p_2 \\ \Delta q \end{pmatrix} = \begin{pmatrix} \cos\varphi\cos\theta & -\sin\varphi & \cos\varphi\sin\theta \\ \sin\varphi\cos\theta & \cos\varphi & \sin\varphi\sin\theta \\ -\sin\theta & 0 & \cos\theta \end{pmatrix} \begin{pmatrix} \Delta p_{v1} \\ \Delta p_{v2} \\ \Delta q_v \end{pmatrix}, \qquad \text{(A-1)}$$

From eqs. (6) and (7), we obtain the perturbations of the vertical slowness q and q_v, respectively,

$$\Delta q = (\partial q/\partial p_1)\Delta p_1 + (\partial q/\partial p_2)\Delta p_2 \quad , \tag{A-2}$$

$$\Delta q_v = (\partial q_v/\partial p_{v1})\Delta p_{v1} + (\partial q/\partial p_{v2})\Delta p_{v2} \quad . \tag{A-3}$$

To represent the slowness derivatives $\partial q_v/\partial p_{v1}$ and $\partial q/\partial p_{v2}$ in a TTI medium in terms of the slowness derivatives $\partial q/\partial p_1$ and $\partial q/\partial p_2$ in a VTI medium, we consider two special cases. For the first case, we assume that the perturbation of the slowness surface in a VTI medium is caused by change in only p_{v1} not p_{v2}, that is

$$\Delta p_{v2} = 10 \quad . \tag{A-4}$$

From eqs. (A-1)-(A-4), we derive a linear system of equations given by

$$\begin{pmatrix} 1 & 0 & -[\cos\varphi\cos\theta + \cos\varphi\sin\theta(\partial q_v/\partial p_{v1})] \\ 0 & 1 & -[\sin\varphi\cos\theta + \sin\varphi\sin\theta(\partial q_v/\partial p_{v1})] \\ \partial q/\partial p_1 & \partial q/\partial p_2 & [\sin\theta - \cos\theta(\partial q_v/\partial p_{v1})] \end{pmatrix} \begin{pmatrix} \Delta p_1 \\ \Delta p_2 \\ \Delta p_{v1} \end{pmatrix} = 0 \quad . \tag{A-5}$$

It follows that the expression for $\partial q_v/\partial p_{v1}$ is given by

$$\partial q_v/\partial p_{v1} = -[(\partial q/\partial p_1)\cos\varphi\cos\theta + (\partial q/\partial p_2)\sin\varphi\cos\theta + \sin\theta]$$
$$/[(\partial q/\partial p_1)\cos\varphi\sin\theta + (\partial q/\partial p_2)\sin\varphi\sin\theta - \cos\theta] \quad . \tag{A-6}$$

For the second case, we assume that the perturbation of the slowness surface in a VTI medium is caused by change in only p_{v2} not p_{v1}, that is

$$\Delta p_{v1} = 0 \quad . \tag{A-7}$$

Similar manipulations are performed for eqs. (A-1)-(A-3) and (A-7), resulting in another linear system of equations,

$$\begin{pmatrix} 1 & 0 & [\sin\varphi - \cos\varphi\sin\theta(\partial q_v/\partial p_{v2})] \\ 0 & 1 & -[\cos\varphi + \sin\varphi\sin\theta(\partial q_v/\partial p_{v2})] \\ \partial q/\partial p_1 & \partial q/\partial p_2 & -\cos\theta(\partial q_v/\partial p_{v2})] \end{pmatrix} \begin{pmatrix} \Delta p_1 \\ \Delta p_2 \\ \Delta p_{v1} \end{pmatrix} = 0 \quad . \tag{A-8}$$

By setting the determinant of coefficient matrix given in eq. (A-8) zero, we derive the expression for $\partial q_v/\partial p_{v2}$,

$$\partial q_v/\partial p_{v2} = [(\partial q/\partial p_1)\sin\varphi - (\partial q/\partial p_2)\cos\varphi]$$

$$/[(\partial q/\partial p_1)\cos\varphi\sin\theta + (\partial q/\partial p_2)\sin\varphi\sin\theta - \cos\theta] \quad . \qquad \text{(A-9)}$$

Eqs. (A-6) and (A-9) give the slowness derivative relations between VTI and TTI media. Similar ideas are used by Stovas and Alkhalifah (2013) for mapping of moveout functions in TI media and Hao et al. (2013) for deriving the slowness derivative relations between VTI and HTI media.

APPENDIX B

ANALYTICAL APPROXIMATIONS FOR SLOWNESS IN VTI MEDIA

To derive the approximate solutions of eqs. (19) and (20), we assume that p_v^2 and q_v^2 can be approximately represented in forms of second-order perturbation with respect to the anellipticity parameter η,

$$p_v^2 = a_0 + a_1(2\eta) + a_2(2\eta)^2 \quad , \qquad \text{(B-1)}$$

$$q_v^2 = b_0 + b_1(2\eta) + b_2(2\eta)^2 \quad . \qquad \text{(B-2)}$$

By substituting eq. (B-1) into equation (19), we determine coefficients a_i, $i = 0,1,2$,

$$a_0 = c^2v_0^2/[v_{nmo}^2(c^2v_0^2 + v_{nmo}^2)] \quad , \qquad \text{(B-3)}$$

$$a_1 = -c^4v_0^4(c^2v_0^2 + 4v_{nmo}^2)/[v_{nmo}^2(c^2v_0^2 + v_{nmo}^2)^3] \quad , \qquad \text{(B-4)}$$

$$a_2 = c^6v_0^6(c^4v_0^4 + 5c^2v_0^2v_{nmo}^2 + 22v_{nmo}^4)/[v_{nmo}^2(c^2v_0^2 + v_{nmo}^2)^5] \quad . \qquad \text{(B-5)}$$

In a similar way, we obtain coefficients b_i, $i = 0,1,2$,

$$b_0 = v_{nmo}^2/[v_0^2(c^2v_0^2 + v_{nmo}^2)] \quad , \qquad \text{(B-6)}$$

$$b_1 = 3c^4v_0^2v_{nmo}^2/(c^2v_0^2 + v_{nmo}^2)^3 \quad , \qquad \text{(B-7)}$$

$$b_2 = 3v_0^4(c^8v_0^2v_{nmo}^2 - 5c^6v_{nmo}^4)/(c^2v_0^2 + v_{nmo}^2)^5 \quad . \qquad \text{(B-8)}$$

Furthermore, Shanks transform (Bender and Orszag, 1978) is employed to improve the accuracy of the perturbation solutions for p_v^2 and q_v^2 and given in eqs. (B-1) and (B-2). The final expressions become

$$p_v^2 = c^2v_0^2[c^6v_0^6 + 4v_{nmo}^6 + 6c^4v_0^4v_{nmo}^2(1-\eta) + 3c^2v_0^2v_{nmo}^4(3+4\eta)]$$

$$/\{v_{nmo}^2(c^2v_0^2 + v_{nmo}^2)[4v_{nmo}^6 + c^6v_0^6(1+2\eta)$$

$$+ 2c^4v_0^4v_{nmo}^2(3+5\eta) + c^2v_0^2v_{nmo}^4(9+44\eta)]\} \quad . \tag{B-9}$$

$$q_v^2 = v_{nmo}^2[v_{nmo}^4 + c^4v_0^4(1+4\eta) + 2c^2v_0^2v_{nmo}^2(1+5\eta)]$$

$$/\{v_0^2(c^2v_0^2 + v_{nmo}^2)[v_{nmo}^4 + c^4v_0^4(1-2\eta) + 2c^2v_0^2v_{nmo}^2(1+5\eta)]\} \quad . \tag{B-10}$$

APPENDIX C

THE EFFECTIVE MEDIUM PARAMETERS FOR A MULTI-LAYERED DTI MODEL

In this appendix, we derive the effective medium parameters for a multi-layered DTI model. We consider the 2D multi-layered DTI model with the symmetry axis assigned in [x,z] plane.

Fig. C-1 shows the propagation of seismic ray in a multi-layered DTI model. From the geometrical relations, we obtain the reflection traveltime T_{dti} for the P-wave in the DTI model given by

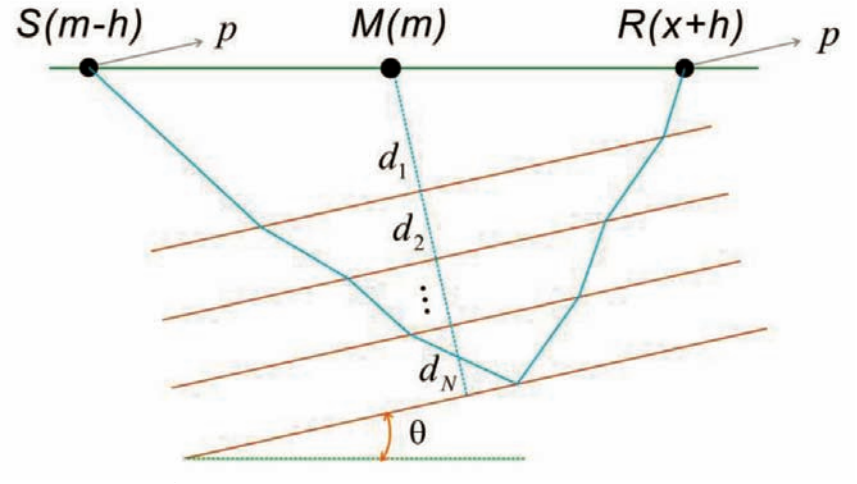

Fig. C-1. Schematic plot of the P-wave reflection in a 2D multi-layered DTI model. In this model, all layer interfaces are parallel to each other. The symmetry axis is normal to all layer interfaces. Symbols M, S and R illustrate midpoint, source and receiver, respectively. m and h denote the lateral position of the midpoint and source-receiver half-offset, respectively. d_i denotes the thickness of the i-th layer. p denotes the projection of the slowness on layer interfaces. θ denotes the dip of the symmetry axis.

$$T_{dti}(h) = 2hp\cos\theta + 2\sum_{k=1}^{N} d_k q_k(p) \quad , \tag{C-1}$$

with

$$h\cos\theta + \sum_{k=1}^{N} d_k(\partial q_k/\partial p)(p) = 0 \quad , \tag{C-2}$$

where h denotes the source-receiver half-offset; d_k denotes the thickness of the k-th layer; N denotes the number of the layers in the DTI model; p denotes the projection of the P-wave slowness on layer interfaces; q_k denotes the k-th layer slowness projection normal to layer interfaces, which is a function of slowness projection p; θ denotes the dip of the symmetry axis.

From eqs. (C-1) and (C-2), we consider a corresponding multi-layered VTI model (see Fig. C-2). We assume that both models have the same medium parameters for each layer and the thickness $\tilde{d}_k$ of the k-th layer in the VTI model is proportional to the thickness d_k of the k-th layer in the DTI model,

$$\tilde{d}_k = d_k/\cos\theta \quad . \tag{C-3}$$

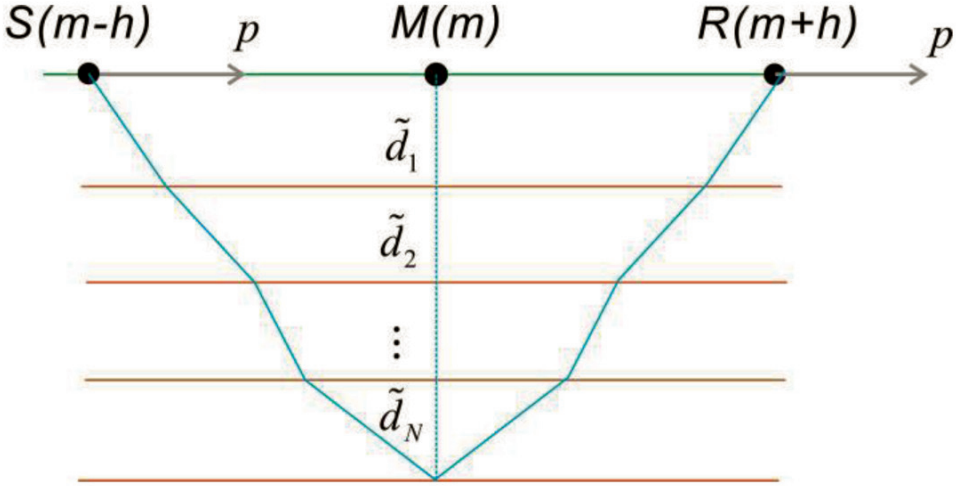

Fig. C-2. Schematic plot of P-wave reflection in a 2D multi-layered VTI model. Symbols M, S and R illustrate midpoint, source and receiver, respectively. m and h denote the lateral position of the midpoint and source-receiver half-offset, respectively. $\tilde{d}_i$ denotes the thickness of the i-th layer. p denotes the projection of the slowness on layer interfaces.

In the multi-layered VTI model, the reflection traveltime for half-offset h is represented by parametric equation,

$$T_{vti}(h) = 2hp + 2\sum_{k=1}^{N} \tilde{d}_k q_k(p) \quad , \tag{C-4}$$

where q_k denotes the vertical projection of the P-wave slowness for the k-th layer in the VTI model; the horizontal slowness component p satisfies

$$h + \sum_{k=1}^{N} \tilde{d}_k(\partial q_k/\partial p)(p) = 0 \quad . \tag{C-5}$$

By comparing eqs. (C-1) and (C-2) with eqs. (C-4) and (C-5) and considering relation (C-3), we obtain

$$T_{dti}(h) = T_{vti}(h)\cos\theta \quad . \tag{C-6}$$

Eq. (C-6) indicates that the P-wave reflection traveltime for the multi-layered DTI model can be obtained from the corresponding multi-layered VTI model, which means that the existing traveltime approximations in VTI media can apply for the multi-layered DTI model, e.g., the rational approximation (Tsvankin, 1994) and generalized moveout approximation (Fomel and Stovas, 2010).

For the P-wave reflection traveltime in the multi-layered VTI model, its moveout expansion with respect to the half-offset h is given by (Ursin and Stovas, 2006),

$$T_{vti}^2(h) = \tilde{\tau}_0^2 + [(2h)^2/v_{nmo}^2] - (2\eta/\tilde{\tau}_0^2 v_{nmo}^4)(2h)^4 + O(h^4) = 0 \quad , \tag{C-7}$$

where two-way zero-offset traveltime $\tilde{\tau}_0$, NMO velocity v_{nmo} and anellipticity η are represented in terms of interval parameters,

$$\tilde{\tau}_0 = \sum_{k=1}^{N} \Delta\tilde{\tau}_{0,k} \quad , \tag{C-8}$$

$$v_{nmo}^2 = (1/\tilde{\tau}_0)\sum_{k=1}^{N} v_{nmo,k}^2 \Delta\tilde{\tau}_{0,k} \quad , \tag{C-9}$$

$$\eta = (1/8)[1/(\tilde{\tau}_0 v_{nmo}^4)]\sum_{k=1}^{N} v_{nmo,k}^4 \Delta\tilde{\tau}_{0,k}(1+8\eta_k) - (1/8) \quad , \tag{C-10}$$

with

$$\Delta\tilde{\tau}_{0,k} = 2\tilde{d}_k/v_{0,k} \quad . \tag{C-11}$$

Here $\Delta\tilde{\tau}_{0,k}$ denotes the two-way zero-offset traveltime for the k-th VTI layer; $v_{0,k}$, $v_{nmo,k}$, η_k are the on-symmetry axis velocity, NMO velocity and anellipticity for the k-th VTI layer, respectively.

It is known that the moveout expansion for a single homogeneous VTI layer can also be written in the form like eq. (C-7). If we treat this multi-layered VTI model as an effective homogenous VTI medium, NMO velocity v_{nmo} given in eq. (C-9) and anellipticity η given in eq. (C-10) can be viewed as the corresponding effective parameters. From eqs. (C-8) and (C-11), we can also obtain the on-symmetry-axis velocity v_0 for this effective VTI medium,

$$v_0 = \sum_{k=1}^{N} \tilde{d}_k \Big/ \sum_{k=1}^{N} (\tilde{d}_k/v_{0,k}) \quad , \tag{C-12}$$

From the reflection traveltime relation (C-6) and the moveout expansion (C-7) for P-wave in the multi-layered VTI model, it follows that the moveout expansion for the multi-layered DTI model is written as

$$T_{vti}^2(h) = \tilde{\tau}_0^2 + [(2h\cos\theta)^2/v_{nmo}^2] - [2\eta/(\tilde{\tau}_0^2 v_{nmo}^4)](2h\cos\theta)^4 + O(h^4) = 0 \ , \tag{C-13}$$

where the expressions for the NMO velocity v_{nmo} and anellipticity η are the same as the ones given in eqs. (C-9) and (C-10); the zero-offset two-way traveltime τ_0 is given by

$$\tau_0 = \tilde{\tau}_0\cos\theta = \sum_{k=1}^{N} \Delta\tau_{0,k} \quad , \tag{C-14}$$

with

$$\Delta\tau_{0,k} = 2d_k/v_{0,k} \quad . \tag{C-15}$$

Here $\Delta\tau_{0,k}$ denotes the zero-offset two-way traveltime for the k-th layer in the multi-layered DTI model.

If we view the product $h\cos\theta$ given in eqs. (36) and (37) with $\gamma = \varphi$ as a single parameter, it is easy to verify that the moveout expansion for P-wave in a 2D homogeneous DTI model can also be written in the same form as the moveout expansion (C-13) for the multi-layered DTI model. Therefore, from these equivalent relations mentioned above, we conclude that the effective medium parameters for the multi-layered DTI model are the same as the ones for the multi-layered VTI model and can be represented in terms of the interval parameters of the multi-layered DTI model,

$$v_0 = \sum_{k=1}^{N} d_k \Big/ \sum_{k=1}^{N} (d_k/v_{0,k}) \quad , \tag{C-16}$$

$$v_{nmo}^2 = (1/\tau_0) \sum_{k=1}^{N} v_{nmo0,k}^2 \Delta\tau_{0,k} \quad , \tag{C-17}$$

$$\eta = (1/8)(1/\tau_0 v_{nmo}^4) \sum_{k=1}^{N} v_{nmo,k}^4 \Delta\tau_{0,k}(1+8\eta_k) - (1/8) \quad , \tag{C-18}$$

where the expression for $\Delta\tau_{0,k}$ is given in eq. (C-14).